# Modified Grid Clustering Technique to Predict Heat Transfer Coefficient in a Duct of Arbitrary Cross Section Area

**AbdulKareem Abbas Khudhair**
Lecturer
Mechanical Engineerig Deparemement / U.O.T.
E-mail: karimmosawi@yahoo .com

## ABSTRACT

**A** simple straightforward mathematical method has been developed to cluster grid nodes on a boundary segment of an arbitrary geometry that can be fitted by a relevant polynomial. The method of solution is accomplished in two steps. At the first step, the length of the boundary segment is evaluated by using the mean value theorem, then grids are clustered as desired, using relevant linear clustering functions. At the second step, as the coordinates cell nodes have been computed and the incremental distance between each two nodes has been evaluated, the original coordinate of each node is then computed utilizing the same fitted polynomial with the mean value theorem but reversibly.

The method is utilized to predict Nusselt number distribution in a hybrid cross section area duct, non-circular non-rectangular, for laminar incompressible flow under Uniform Wall Temperature condition. The results have been compared with the published data and the agreement has been found very well.

**Key words:** heat transfer, grid generation, clustering.

# طريقة مطورة لتنضيد العقد لغرض التنبؤ بمعامل انتقال الحرارة على طول مجرى ذو مقطع مساحة اعتباطي

**عبد الكريم عباس خضير**
مدرس
قسم الهندسة الميكانيكية / الجامعة التكنولوجية

## الخلاصة

تم تطوير طريقة رياضية مباشرة لتنضيد العقد على قطعة حد منحنية ذات شكل اعتباطي بشرط انه يمكن تمثيل قطعة الحد هذه باستعمال متطابقة متعددة الحدود مناسبة. تتكون طريقة الحل بشكل عام من مرحلتين. الأولى تتمثل بتحويل قطعة الحد هذه الى قطعة مستقيم وايجاد طولها باستخدام نظرية متوسط القيمة. ثم نقوم بتوزيع العقد على قطعة المستقيم باستخدام طرق التنضيد الملائمة. وتتمثل المرحلة الثانية بإرجاع المستقيم الى أصله كقطعة خط منحني بعد ان تمت معرفة احداثيات العقد والمسافات بينها بالاستفادة من متطابقة متعددة الحدود نفسها ونظرية متوسط القيمة ولكن بشكل معكوس.

استخدمت الطريقة لإيجاد توزيع عدد نسلت على طول مجرى ذو مقطع هجين غير دائري وغير مستطيل لجريان طباقي غير انضغاطي وتمت مقارنة النتائج مع البيانات المنشورة وكان التطابق جيد جدا.

## 1. NTRODUCTION

For computational fluid dynamics problems, grid clustering in regions of high gradients of variables is of vital importance. It is obvious that one of the most regions of high gradients is at the vicinity of wall.

For a straight-line boundary segment such as rectangular cross section duct inlet, room walls …etc., the clustering is straightforward and linear clustering functions are available in many related CFD books. For example Robert in 1971 proposed a family of general stretching transformations, **Tannehill, et al., 1997**, represented a set of linear clustering functions. Some of these clustering functions are adapted here.

Usually grids clustering are made along a straight line (along one Cartesian axis) by adapting one of the linear cluster function. For curved segment, nodes have a variable x, y coordinates and these cluster function are not applicable directly.

Generally, and especially for strongly curved segments, it is not convenient to approximate the curved boundary as a straight line. For example when solving for flow around an airfoil, airfoil cannot be approximate as a rectangular.

Now days, the majority of CFD researchers are using a commercial CFD package to generate grids externally and internally for curved geometries and solving for flow variables. The body fitted coordinate system is the default coordinates system used to describe such geometries.

But for researchers who are interest in programming the governing equations rather using a commercial CFD package will face a real problem in clustering for such curved segments.

A simple procedure is suggested, developed and presented here to cluster grids along boundary segment of an arbitrary geometry. The method is utilized to predict Nusselt number distribution along a duct of hybrid cross section area for laminar incompressible flow under uniform wall temperature condition. The cross section area is quadrilateral which consists of two straight segments and two curved segments. The results were compared with the published data.

## 2. MATHEMATICAL REPRESENTATION.

The following stretching function is preferable in s-direction for a straight line, **Tannehill, et al., 1997**, which clusters grids towards segment ends:

$$\eta = \alpha + (1-\alpha) * \ln \frac{\{\beta + [s(2\alpha+1)/L] - 2\alpha\}}{\{\beta - [s(2\alpha+1)/L] + 2\alpha\}} \Big/ \ln[(\beta+1)/(\beta-1)] \qquad (1)$$

Eq. (1) describes the clustering in the computation domain. It must be inverted in order to express ($s$) as a function of ($\eta$) in the physical domain, as:

$$\frac{(\eta-\alpha)}{(1-\alpha)} ln[(\beta+1)/(\beta-1)] = ln \frac{\{\beta + [s(2\alpha+1)/L] - 2\alpha\}}{\{\beta - [s(2\alpha+1)/L] + 2\alpha\}}$$

$$[(\beta+1)/(\beta-1)]^{\frac{(\eta-\alpha)}{(1-\alpha)}} = \{\beta + [s(2\alpha+1)/L] - 2\alpha\}/\{\beta - [s(2\alpha+1)/L] + 2\alpha\}$$

let $A = [(\beta+1)/(\beta-1)]^{\frac{(\eta-\alpha)}{(1-\alpha)}}$ (2)

$A\{\beta - [s(2\alpha+1)/L] + 2\alpha\} = \{\beta + [s(2\alpha+1)/L] - 2\alpha\}$

$A(\beta+2\alpha) - (\beta-2\alpha) = (A+1)[s(2\alpha+1)/L]$

$$s = L\frac{A(\beta+2\alpha)-(\beta-2\alpha)}{(A+1)(2\alpha+1)} \qquad (3)$$

The stretching parameter $(\beta)$ has a numeric value which is slightly above unity, $\beta = 1.01\ to\ 1.2$ and it controls the grids refining intensity. $(\eta)$ in Eq. (3) is a counter from $(1\ to\ NJ)$. $(NJ)$ is the number of grids along the segment in $\eta$-direction. $(L)$ is the length of this straightened segment. Then $(s)$ represent the incremental distance between two successive grids along $\eta$-direction.

In this transformation, the clustering parameter $(\alpha)$ is a numeric constant, which is chosen to refine grids near segment ends. If $(\alpha = 0)$, grids will be refined near segment end where $(\mathrm{J} = NJ)$ and if $(\alpha = 1)$, grids will be refined near segment end where $(\mathrm{J} = 1)$, see **Fig. 1**.

For two-dimensional flow between two parallel plates, grids need to be clustered equally near solid boundaries so the clustering parameter is usually taken to be $(\alpha = 0.5)$, and Eq. (2) becomes:

$$s = L\frac{A(\beta+1)-(\beta-1)}{2(A+1)} \qquad (4)$$

Eq. (4) is used to cluster grids along ($\eta$ -coordinate). For the computation domain, usually $\Delta\eta$ has a numeric value of unity, but in the physical domain $\Delta\eta = s$.

For a straight-line segment, Eq. (4) is applied directly. But For curved segment, the linear clustering cannot be applied directly. So a mathematical manipulation to the curved segment should be executed. The segment is first straightened mathematically and its exact length is computed, and then Eq. (4) is applied.

According to mean value theorem, **George,** and **Ross, 1998**, which states" if $y = f(x)$ is continuous at each point of [a, b] and differentiable at each point of [a, b], then there is at least one tangent (g) between (a) and (b) for which, see **Fig. 2**.

$$\frac{f(x_2)-f(x_1)}{x_2-x_1} = \acute{f}(g) \qquad (5)$$

The curved segment $(PQ)$ is approximated by a straight line, which length equals $\sqrt{(\Delta x)_j^2 + (\Delta y)_j^2}$, so the overall length of the curved segment (ab) is;

$$L \cong \sum_{J=1}^{n}\sqrt{(\Delta x)_J^2 + (\Delta y)_J^2} \qquad (6)$$

$$L = \lim_{n\to\infty} \sum_{J=1}^{n} \sqrt{(\Delta x)_j^2 + (\Delta y)_J^2} \qquad (7)$$

The slope of line ($PQ$) is approximate by;

$$\acute{f}(g) = \Delta y / \Delta x \qquad (8)$$

$$\Delta y = \Delta x \, \acute{f}(g) \qquad (9)$$

Then Eq. (7) becomes: -

$$L = \lim_{n\to\infty} \sum_{J=1}^{n} \sqrt{(\Delta x)_j^2 + \left(\Delta x \, \acute{f}(g)\right)_J^2}$$

Then;

$$L = \int_a^b \sqrt{1 + \left(\acute{f}(g)\right)_J^2} \, dx \qquad (10)$$

The segment end points $a(x, y)$ and $b(x, y)$ are prescribed in advance while segment equation, $y = f(x)$, either known or a relevant, simple polynomial is fitted to the curved boundary segment.

Segment length ($L$) is evaluated from Eq. (10) and the number of grids is decided then Eq. (4) is used to cluster grids along the straightened boundary. The incremental distance, ($s$), distribution is computed.

Substitute each incremental distance length and the starting point ($x$) value, starting from point ($a(x, y)$) as input data, in the solution of Eq. (10). Then the value of ($x$) for each ending point is evaluated, since this equation has the ($x$) variable only. The ($NJ - 2$) number of linear Equations are solved by (Do …. ENDDO) loop.

The calculated value of ($x$) is then substituted into segment equation ($y = f(x)$) to determine the ($y$) value for the corresponding point. The final result is a desirable well-clustered curved segment.

To demonstrate the beneficial of the method, let consider a common example which is simple and popular. For a circular arc shape segment of constant radius ($R$), the arc is described by the following special polynomial equation:

$$x^2 + y^2 = R^2 \qquad (11)$$

$$y = (R^2 - x^2)^{1/2}$$

$$\acute{y} = 0.5(R^2 - x^2)^{-0.5}(-2x)$$

$$\acute{y} = -x/\sqrt{R^2 - x^2} \qquad (12)$$

Substitute for the slope ($\acute{f}(g)$) from Eq. (12) in to Eq. (10) , then the length ($L$) becomes;

$$L = \int_a^b \sqrt{1 + \left(-x/\sqrt{R^2 - x^2}\right)^2}\, dx \qquad (13)$$

$$= \int_a^b \left(\frac{R^2}{(R^2 - x^2)}\right)^{0.5} dx$$

$$= R\int_a^b \frac{1}{(R^2 - x^2)^{0.5}}\, dx \qquad (14)$$

.

To interpret from Cartesian to polar coordinate system, precede as;

$$x = R\cos\theta$$

$$dx = -R\sin\theta\, d\theta$$

$$R^2 - x^2 = R^2 - R^2\cos^2\theta$$

$$R^2 - x^2 = R^2(1 - \cos^2\theta)$$

$$= R^2\sin^2\theta \qquad (15)$$

Substitute from Eq. (15) into Eq. (13) gives;

$$L = R\int_{\theta_a}^{\theta_b} \frac{-R\sin\theta\, d\theta}{(R^2\sin^2\theta)^{0.5}}$$

$$= -R\int_{\theta_b}^{\theta_b} d\theta$$

$$L = R(\theta_b - \theta_a)$$

$$= R\left(\theta_{J=NJ} - \theta_{\mathrm{J=1}}\right) \qquad (16)$$

Eq. (16) is well-known, **George,** and **Ross, 1998**. ($\theta_a$) is the starting angle of the arc in radius at ($J = 1$) and ($\theta_b$) is the ending angle of the arc in radius at ($J = NJ$). These two ends angle are prescribed in advance.

Substituting the value of arc length ($L$) from Eq. (16) into Eq. (4), then the length of sub-division segment ($s_J$) is evaluated directly. Rearrange Eq. (16) to compute the end segment angle ($\theta_J$) in terms of the start sub-division segment angle ($\theta_{J-1}$) and it length ($s_J$), as;

$$\theta_J = \theta_{J-1} - \frac{s_J}{R} \qquad (17)$$

Now all nodes angle, $\theta_1, \theta_2, \theta_£, \dots\ \theta_{NJ}$, are computed and ($R$) is constant then, the value of ($x$) and ($y$) for each node are evaluated directly as:

$$x_J = R\cos\theta_J \ \ ; \ \ y_J = R\sin\theta_J \qquad (18)$$

At this stage grids are distributed externally along the boundaries nicely and as needed. The internally grid distribution is accomplished by using the TTM Poisson type method, **Thompson, et al., 1985**. The TTM method, named due to (Thompson, Thames, and Mastin ), with an essential contribution from (Thomas, and Middlecoff), **Thomas, 1980**, **Thomas, et al., 1982**. The TTM method is the corner stone of grid generation techniques now days, **Thompson, 2000**. **Fig. 6** shows two types of internally grid generation depending on the external grids distribution.

The details of the TTM method for internally grid generation is prescribed by **Khudhair, 2003.**

## 3. HEAT TRANSFER APPROACH.

To demonstrate the validity of the method, a convective heat transfer coefficient was evaluated in a duct of non-circular and non-rectangular cross section as shown in **Fig. 3**.

Unfortunately neither the Cartesian nor the cylindrical coordinate system is a proper choice for such cross section. The body fitted coordinate system is convenient system. So the fluid governing equations will be first written in a Cartesian coordinate system and then transferred to a body fitted coordinate system.

The governing equations in Cartesian coordinate system for steady, incompressible, three-dimensional laminar flow with constant specific heats are, **Tannehill, et al., 1997**:

$$\nabla.\left(\rho\vec{\boldsymbol{V}}\right) = 0 \qquad (18)$$

$$\nabla.\left(\rho u\vec{\boldsymbol{V}}\right) = -\frac{\partial p}{\partial x} + \nabla.(\mu\nabla.u) + S_{Mx} \qquad (19a)$$

$$\nabla.\left(\rho v\vec{\boldsymbol{V}}\right) = -\frac{\partial p}{\partial y} + \nabla.(\mu\nabla.v) + S_{My} \qquad (19b)$$

$$\nabla.\left(\rho w\vec{\boldsymbol{V}}\right) = -\frac{\partial p}{\partial z} + \nabla.(\mu\nabla.w) + S_{Mz} \qquad (19c)$$

$$\nabla.\left(\rho T\vec{\boldsymbol{V}}\right) = \nabla.(\mu\nabla.T) + S_T \qquad (20)$$

These governing equations are in Cartesian coordinate system, which is not convenient to solve for a flow inside a duct with arbitrary cross section area. Also the polar coordinate is not convenient for a cross section area as shown by **Fig. 5**. The body fitted coordinate system is the convenient choice. Details of transformation to body fitted coordinate system and discretization for continuity, momentum and energy equations are presented in details by **Khudhair, 2003, 2013**.

From **Fig. 4**, the increase or decrease of heat within the control is equal to the heat gained or lost by convection through duct wall, i.e.

$$\delta Q_{C.V.} = \delta Q_{conv} \qquad (21)$$

$$\dot{m}c_p dT = h_j P dx\left(T_w - T_{f,j}\right) \qquad (22)$$

Since $T_w$ is constant, then;

$$dT = d\left(T_w - T_{f,j}\right)$$

and Eq. (22) becomes:

$$h_j = -\frac{\dot{m}c_p dT}{P dx\left(T_w - T_{f,j}\right)}$$

$$h_j = \frac{\dot{m}c_p}{A_s}\ln\frac{\left(T_w - T_{f,j+1}\right)}{\left(T_w - T_{f,j}\right)} \qquad (23)$$

or simply;

$$\dot{m}c_p \Delta T = h_j A_s\left(T_w - T_{f,j}\right)$$

$$h_j = \frac{\dot{m}c_p\left(T_{f,j+1} - T_{f,j}\right)}{A_s\left(T_w - T_{f,j}\right)} \qquad (24)$$

Eqs. (23) and (24) for local heat transfer coefficient have been programed and solved and they have given ave an identical results. $T_f$ represents the local fluid mean temperature within the control volume between two successive sections.

The local bulk temperature $T_b$, which is the fluid average temperature at each duct section, is evaluated from the conservation of energy. At each cross section, $J$, the number of cells equals $(NI - 1) \times (NK - 1)$.

$$\dot{m}_j c_p T_{b,j} = \sum \dot{m}_{i,j,k} c_p T_{i,j,k}$$

$$= \sum \rho c_p \left( V_{i,j,k} A_{i,j,k} T_{i,j,k} \right) \qquad (25)$$

For the duct under consideration, the cross section area and sectional mean velocity are constant, then.

$$\therefore T_{b,j} = \frac{\sum \left( V_{i,j,k} A_{i,j,k} T_{i,j,k} \right)}{V_m A_C} \qquad (26)$$

The variables $V_{i,j,k}$ and $T_{i,j,k}$ are the output data from the flow governing equation after the solution is converged while $A_{i,j,k}$ is computed from tensor mathematic during grid generation stage.

The local Nusselt number is then evaluated as;

$$Nu_j = \frac{h_j D_j}{k} \qquad (27)$$

$D_j$ is a length scale which is usually taken as the hydraulic diameter. For the case under consideration the hydraulic diameter is constant.

$$D_j = \frac{4A_{cross}}{P} \qquad (28)$$

The average convective heat transfer coefficient depends on the average bulk temperature, which can be interpreted as;

$$T_{b,mean} \sum \dot{m}_j c_p = \sum \dot{m}_j c_p T_{b,j} \qquad (29)$$

Heat transfer coefficient or Nusselt number are usually plotted along the duct length, $x$, in terms of the inverse Graetz number which is a non-dimensional number.

$$Graetz\ number, Gr = Re\, Pr \frac{D_j}{x} \qquad (30)$$

Where Reynolds and Prandtl numbers are define as

$$Re = \frac{\rho V_m D_j}{\mu} \quad ; \quad Pr = \frac{\nu}{\alpha} = \frac{c_p \mu}{k} \qquad (31)$$

## 4. DUCT GEOMETRY.

Firstly, the duct geometry has been drawn programmatically using FORTRAN 90 code. **Fig. 5** shows the duct cross section area, which represents a quadrilateral entry. It consists of two straight walls and two curved walls. Number of grids chosen is $(15 \times 15 \times 501)$. The pipe cross section geometry is not convenient neither for Cartesian coordinate system nor for polar coordinate system and the body fitted coordinate system is the best choice. Grids are distributed automatically as desire directly from Eq. (4) for the straight walls while for the curved walls the grids are distributed entirely following the prescribed procedure as follow:

1. Compute arc length of curved walls from Eq. (16), as $\theta_1$and $\theta_{NJ}$ are known.
2. Cluster grids along the segment ab and cd as desire using Eq. (4).
3. The output of Eq. (4) is the interval distance ($s_J$) between each two successive nodes, which represent the interval arc length.
4. Recalculate ($\theta$) distribution, starting from ($J = 2$) to ($J = NJ - 1$), from Eq. (17).
5. Finding grid node coordinates from Eq. (18).
6. Internally grid generating using the $TTM$ method.

## 5. INPUT DATA.

The working fluid is air with the specifications, which was considered at ($325\ K$), presented in **Table (1)**.

## 6. CODE CONSTRUCTION.

All the related equations have been programed using a FORTRAN 90 programing language. The corestone of the code was developed earlierby **Khudhair, 2003**, and it is modified later to handle the heat transfer problem and the forementioned modification.

## 7. SOLUTION PROCEDURE.

The solution procedure is illustrated in the provided flow chart, **Chart. (1)**.

## 8. RESULT AND DISCUSSION.

**Fig. 7** shows the local Nusselt number distribution along the proposed duct with cluster and uniform grid distribution. The result were compared with the data presented by **Holman, 2010**. Clustering is important at region of high gradient. At the developing entrance region the agreement between predicted with cluster and comparator data is excellent over that uniform grid distribution. At the developed region where temperature and velocity distribution profile is settled, the advantage of clustered over uniform grid generation is vanished and both distribution are in a good agreement with the comparator data.

**Fig. 8** shows the average Nusselt number distribution. The agreement between predicted result with **Holman, 2010,** and the empirical formula proposed by Hausen is very good with $+6.7\%$ and $-4.3\%$ error for uniform and clustered grids respectively, except at the very beginning of entry which may interpreted to the assumed uniform velocity profile at entry. The Hausen empirical relation for fully developed laminar flow for circular tubes at constant wall temperature, presented by **Holman, 2010,** which based on hydraulic diameter, is:

$$\overline{Nu} = 3.66 + \frac{0.0668(d/L)RePr}{1 + 0.04(d/L)RePr^{2/3}}$$

Uniform grid distribution gives fair agreement especially at developing region where high gradients are expected.

## 9. CONCLUSION.

Distribution grid nodes along a curved wall segment is important for thermo-problems. The described method is a mathematical dependent and well programed. Distribution grids along straight wall segment is straight forward. And can be find in many CFD books.

Grid clustering near wall is of vital importance for internal flows in confined conducts or external flows over plates where high gradients are exist. But uniform grid distribution works well when these gradients moderated. At the fully developed region where variables profile is constant, uniform distribution performs better since the cell skewness is greatly reduced.

The proposed technique predicted Nusselt number distribution very well in such conductor with a non-rectangular, non-circular cross section area. As expected the value of Nusselt number at entry has the maximum value where velocity and temperature gradients are high and these values fall down temperature profile settled.

At the end of the duct the predicted average Nusselt number value for clustered grid distribution equals (4.134) with error value of ($-4.3\%$) when compare with Hausen predicted method. While for uniform grid distribution the average Nusselt number value at duct end is (3.698) with error value of ($+6.68$).

The technique presented here is aimed for those who are interest in programming their problem rather using commercial CFD package.

## REFERENCES.


- Al-Dabagh, A. M., Al-Musawi, A. A. and Salam, A. Q., 2012, *Experimental and numerical study of enhancement heat transfer in twisted tubes heat exchangers*, Special Issue of Engineering and Development Journal, ISSN 1813-7822, pp 194-215.

- George B. T., and Ross, L. F.,1998, Calculus and Analytic Geometry, 9th ed, Addison-Wesly Publishing Company.

- Holman J.P., 2010, Heat transfer, 10th ed, The McGraw-Hill companies, Inc.

- Khudhair, A. A. 2013, Twist Parameter Influence on Heat Transfer Coefficient Augmentation for Square Twisted Tube, Engineering & Technology Journal, Vol. 31, part A, No. 9, pp 1802-1819.

- Khudhair, A. A., 2003, Computational Fluid Dynamics with Particular Reference to Centrifugal Pump Impellers. Ph .D. thesis. Mechanical Engineering Department, University of technology.

- Mohammed, A. A., Mohammed, B. A., and Muhee, R. J., 2014, Heat Transfer Enhancement in a Tube Fitted with Nozzle-Turbulators, Perforated Nozzle Turbulators with Different hole shap, Enginnering and Technology, Vol. 32, Part A, No. 10, pp 2514-2527.

- Tannehill, J. C., Anderson, D. A., and Pletcher, R. H., 1997, Computational Fluid Mechanics and Heat Transfer, 2nd editin, Hemisphere publishing corporation, Taylor & Francis group, New York.

- Thomas, P. D. and Middlecoff, J. F., 1980, Direct control of the grid point distribution in meshes generated by elliptic equations, AIAA J., vol. 18, no. 06, pp. 652-656.

- Thomas, P. D., 1982, Composite three-dimensional grid generated by elliptic systems. AIAA J., vol. 20, no. 09, pp. 1195-1202.

- Thompson, J. F., 2000, A Rreflection on Grid Generation in the 90's; Trends, Needs and Influences, Mississippi State University, Mississippi State, MS 39762 USA. Joe Thompson, joe @ erc.msstate.edu.


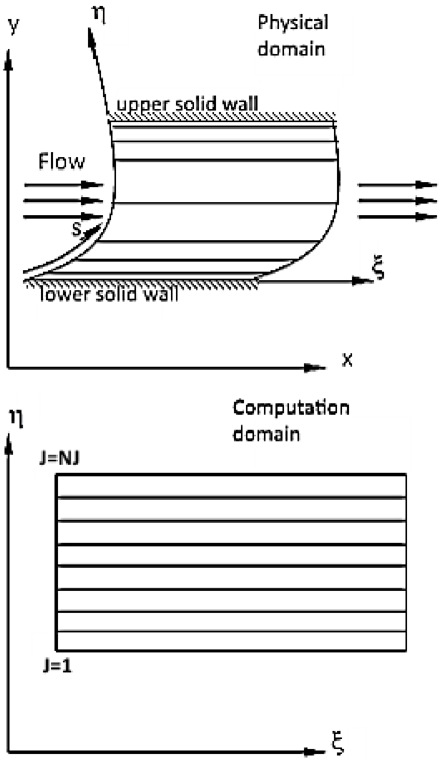


**Figure 1.** Pysical and computation domain


- Thompson, J. F., Warsi, Z. U. A., and Mastin, c. W., 1985, Numerical grid generation, foundations and applications, Elsevier Science Publishing Co., Inc.


## NOMENCLATURE

| | | | | | |
|---|---|---|---|---|---|
| Ac | cross section. | $m^2$ | k | condictivity. | $W/m.℃$ |
| As | surface area. | $m^2$ | L | segment length. | m |
| $c_p$ | specific heat. | $kJ/kg.℃$ | $\dot{m}$ | mass flow rate. | $kg/m^3$ |
| D | hydraulic diameter. | m | Nu | nusselt number. | |
| H | heat transfer coefficient. | $W/m^2.℃$ | P | perimeter. | m |

| | | |
|---|---|---|
| p | pressure. | $N/m^2$ |
| Pr | prandtl number. | |
| R | arc radius. | m |
| Re | reynolds number. | |
| s | incremental distance. | m |
| $S_M$ | source term. | $N/m^3$ |
| $S_T$ | source term. | kg. ℃/s |
| T | temperature. | ℃ or K |
| u | velocity components. | m/s |
| v | velocity components. | m/s |
| V | velocity. | m/s |
| $\vec{V}$ | velocity vector. | m/s |
| w | velocity components. | m/s |
| X | cartesian coord. system. | |
| Y | cartesian coord. system. | |
| Z | cartesian coord. system. | |
| α | clustering parameter. | |
| β | streching parameter. | |
| η | coord. along boundary. | |
| θ | angle. | radian |
| μ | dynamic viscosity. | kg/m. s |
| ν | kinematic viscosity. | $m^2/s$ |

**Table 1**. Inlet air specifications, input data and duct size

| | |
|---|---|
| Air density, $\rho$ | 1.088 $kg/m^3$ |
| Specific heat, $c_p$ | 1007.4 $J/kg.K$ |
| Dynamic viscosity, $\mu$ | $1.96 \times 10^{-5}$ $kg/m.s$ |
| Air condictivity, $k$ | 0.028 $W/m.K$ |
| Prandtl number | 0.705 |
| Inlet air temperature | 25 ℃ |
| Wall temperature | 50 ℃ |
| Bulk velocity | 0.4184 $m/s$ |
| Reynolds number | 1000 |
| Cross section height | 3.536 $cm$ |
| Cross section width | 5.0 $cm$ |
| Duct length | 600 $cm$ |

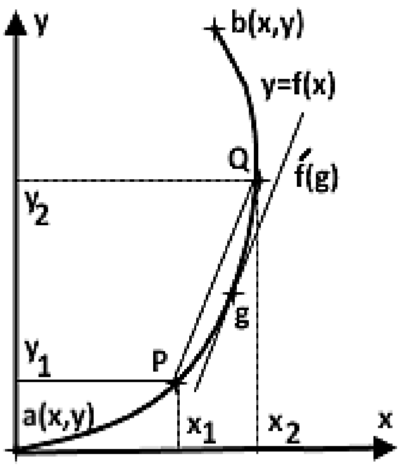


**Figure 2.** Mean value theorm

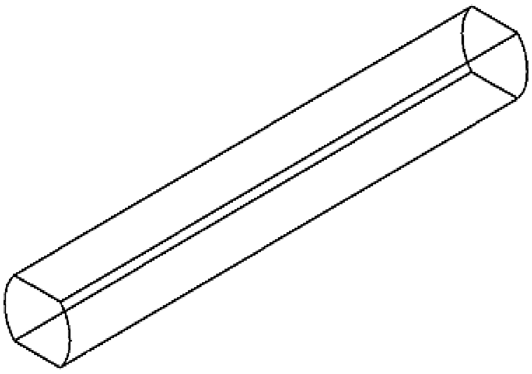

**Figure 3.** Non-circular and non-rectangualar cross section duct.

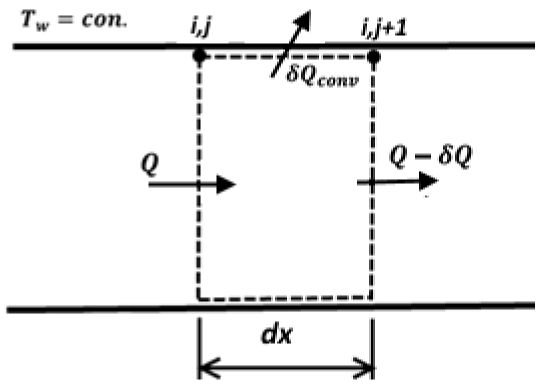


**Figure 4.** Control volume inside the duct

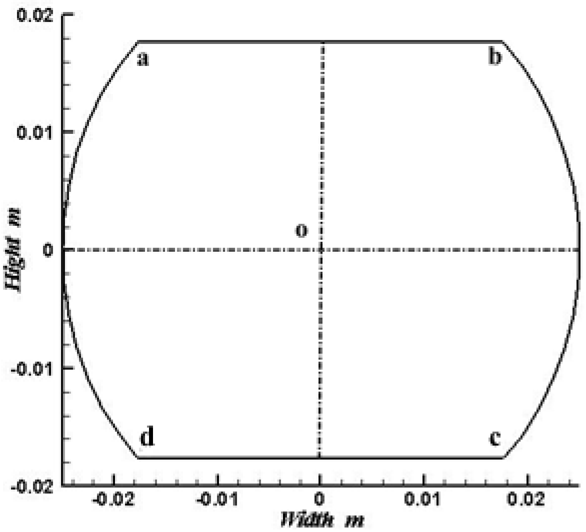


**Figure 5.** Duct cross section area

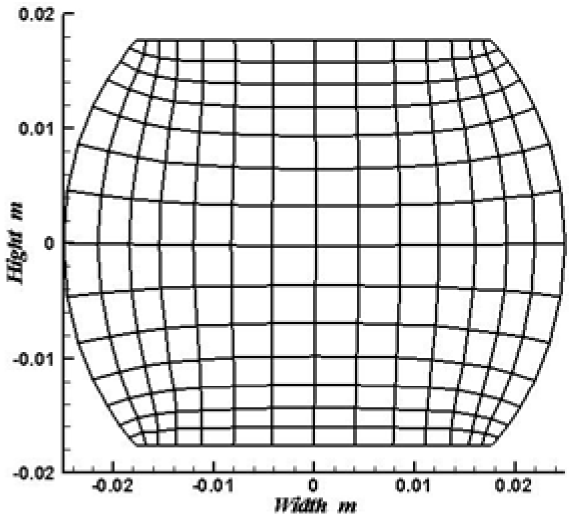


**Figure 6a.** Modify grid clustering

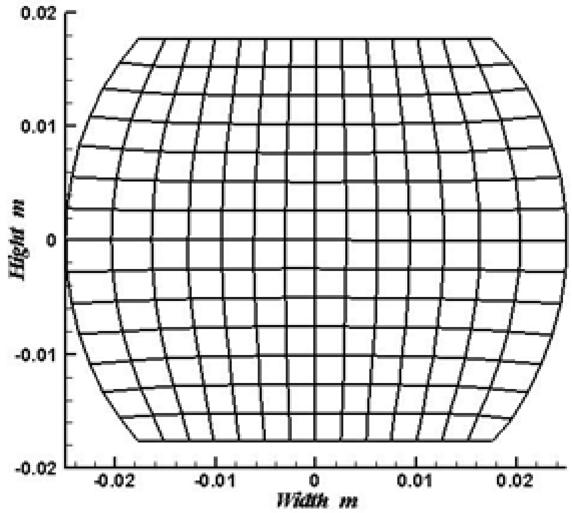


**Figure 6b.** Uniform grid Clustering

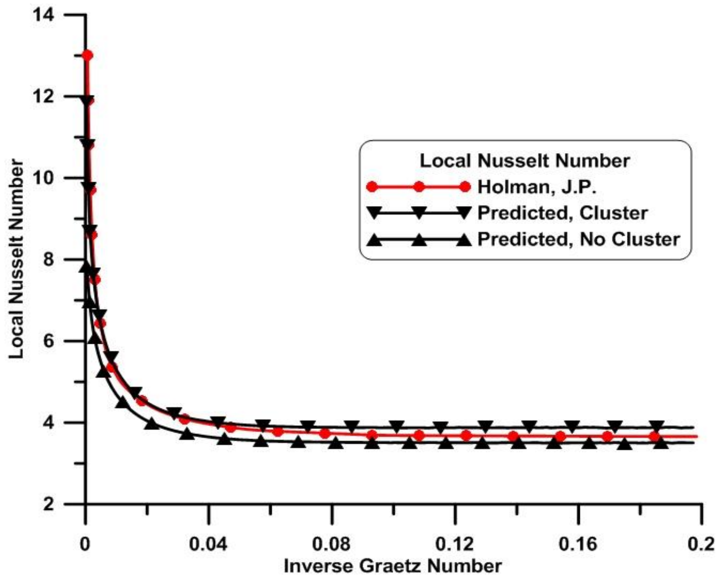


**Figure 7.** Local Nusselt number distribution

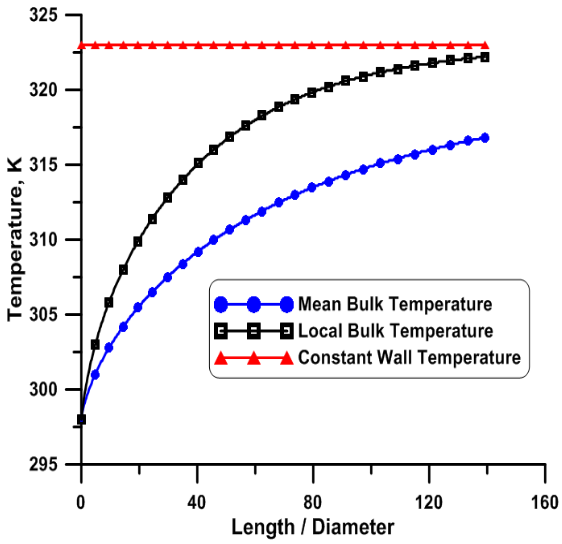


**Figure 10.** Bulk temperature

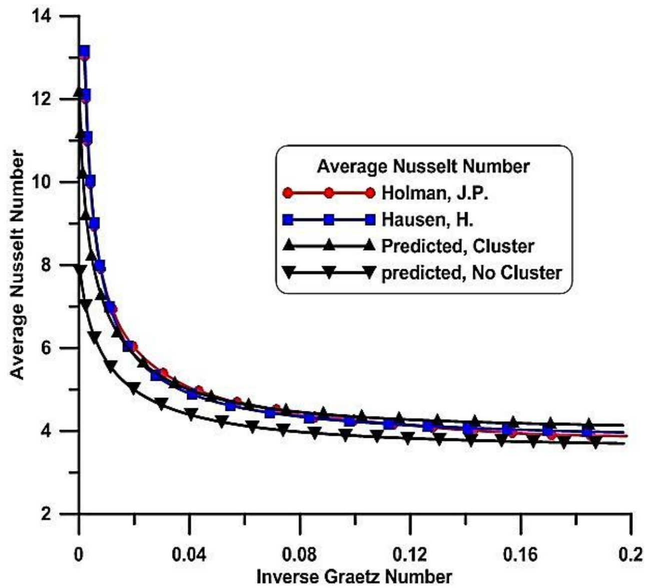


**Figure 8.** Average Nusselt number distribution

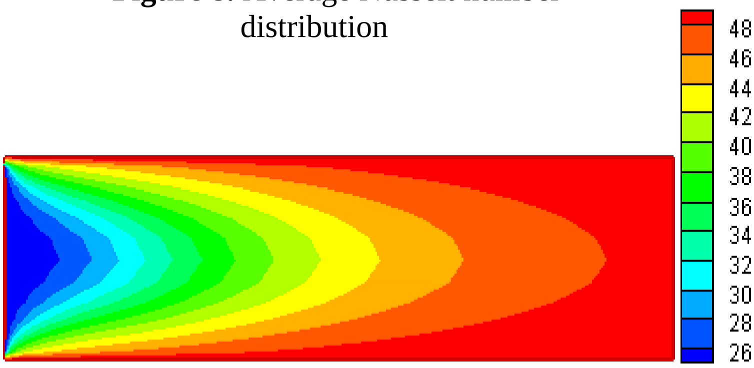

**Figure 9.** Temperature contors at longitudinal mid-section.

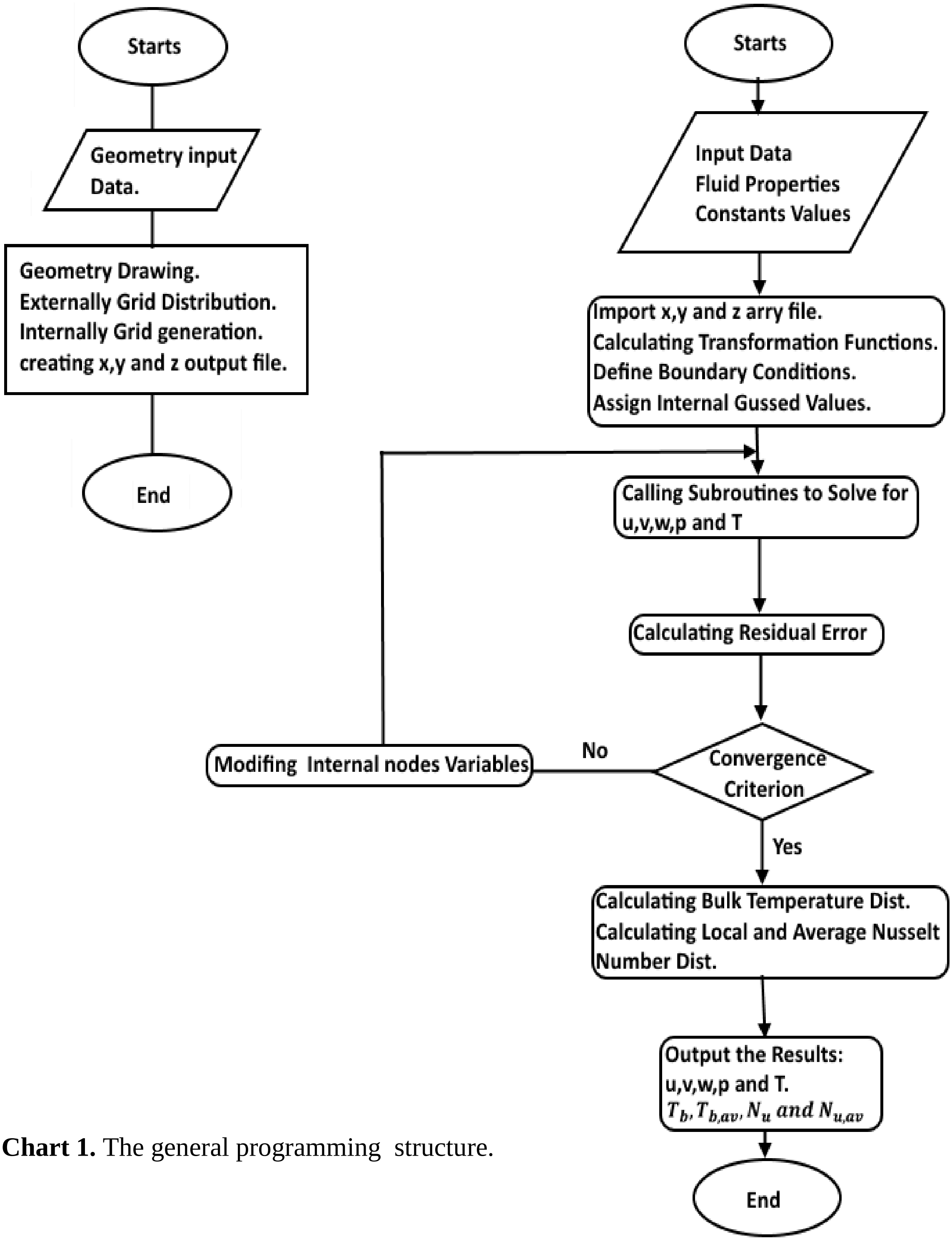


**Chart 1.** The general programming structure.